THE JOURNAL OF PHYSICAL CHEMISTRY Letters

Letter

pubs.acs.org/JPCL

Exciton Structure and Energy Transfer in the Fenna–Matthews–Olson Complex

Erling Thyrhaug,[†] Karel Žídek,[†] Jakub Dostál,[†,‡] David Bína,[§] and Donatas Zigmantas*[,†]

[†]Department of Chemical Physics, Lund University, P.O. Box 124, 22100 Lund, Sweden

[‡]Institut für Physikalische und Theoretische Chemie, Universität Würzburg, Am Hubland, D-97074 Würzburg, Germany

[§]Biology Centre CAS, Branišovská 31, and Faculty of Science, University of South Bohemia, Branišovská 1760, 370 05 České Budějovice, Czech Republic

Supporting Information

ABSTRACT: The Fenna–Matthews–Olson (FMO) photosynthetic complex found in green sulfur bacteria has over the last decades been one of the favorite "model" systems for biological energy transfer. However, even after 40 years of studies, quantitative knowledge about its energy-transfer properties is limited. Here, two-dimensional electronic spectroscopy with full polarization control is used to provide an accurate description of the electronic structure and population dynamics in the complex. The sensitivity of the technique has further allowed us to spectroscopically identify the eighth bacterio-chlorophyll molecule recently discovered in the crystal structure. The time evolution of the spectral structure, covering time scales from tens of femtoseconds up to a nanosecond, reflects the energy flow in FMO and enables us to extract an unambiguous energy-transfer scheme.

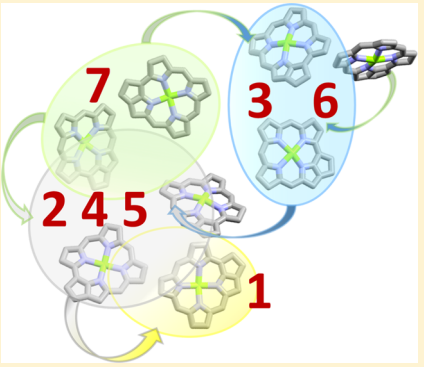

The Fenna–Matthews–Olson (FMO) complex is a small protein homotrimer found in the photosynthetic apparatus of a number of green sulfur bacteria. It was among the first structurally well-characterized photosynthetic proteins and has attracted attention from spectroscopists, theoreticians, and biologists for several decades. The scaffold of the protein supports bacteriochlorophyll *a* (BChl) pigments in a well-defined geometry, shaping its optical properties to appear substantially different from those of the constituent BChl molecules in solution. It is situated between the light-harvesting antenna chlorosome and the photosynthetic reaction center of the bacteria, and due to this positioning and its ladderlike energy-level structure it has been proposed to function as a "funnel" for harvested solar energy toward the reaction center.

Because of the compact and well-known structure, FMO is a convenient and illuminating system to study for both experimentalists and theoreticians. It is water-soluble; its crystal structure has been known in increasing detail since 1975;[1,2] and its relatively small size makes spectral analysis and theoretical modeling *in principle* tractable problems. These advantages have resulted in FMO becoming one of the most thoroughly studied light-harvesting complexes in photosynthetic research.[3] The incentive has been that by understanding the optical properties of this simple system one could achieve greater understanding of the mechanisms of photosynthetic energy transfer in general. However, even in this model system the situation has turned out to be more complicated than initially anticipated, and still, some 40 years after its isolation and characterization, considerable controversy persists about both its function and its fundamental photophysical properties. Exciton energies and their extent of delocalization are still debated, as is both the quantitative and qualitative aspects of energy transfer through the complex. More complex issues, such as the interpretation of quantum beats observed in its time-resolved spectroscopic signals[4−6] have both spurred considerable debate and been among the important factors in initiating the field of quantum biology.

FMO variants from several different species of green sulfur bacteria have been studied in detail, and while some structural and spectroscopic differences are observed, all are C_3 symmetric protein trimers, each unit containing identical structures of 8 BChl pigments (see Figure 1A). One of these, BChl 8, is loosely bound to the protein surface and is typically lost during isolation and purification. As a result, it was only recently discovered in the FMO crystal structure.[2] Some experimental efforts to identify its spectral contribution have been made;[7] however, the majority of work on the optical properties of this BChl have been theoretical,[8−10] where more recent studies suggest that it contributes to the very blue edge of the absorption spectrum.[8]

The *intra*unit electronic coupling among BChl pigments in the protein is moderate (up to approximately 100 cm^{-1}).[11−13] The environment-induced perturbations to the optical transitions are also substantial, which in sum results in a structured lowest-energy absorption band, centered at ∼810

Received: March 7, 2016
Accepted: April 15, 2016
Published: April 15, 2016

DOI: 10.1021/acs.jpclett.6b00534
J. Phys. Chem. Lett. 2016, 7, 1653−1660

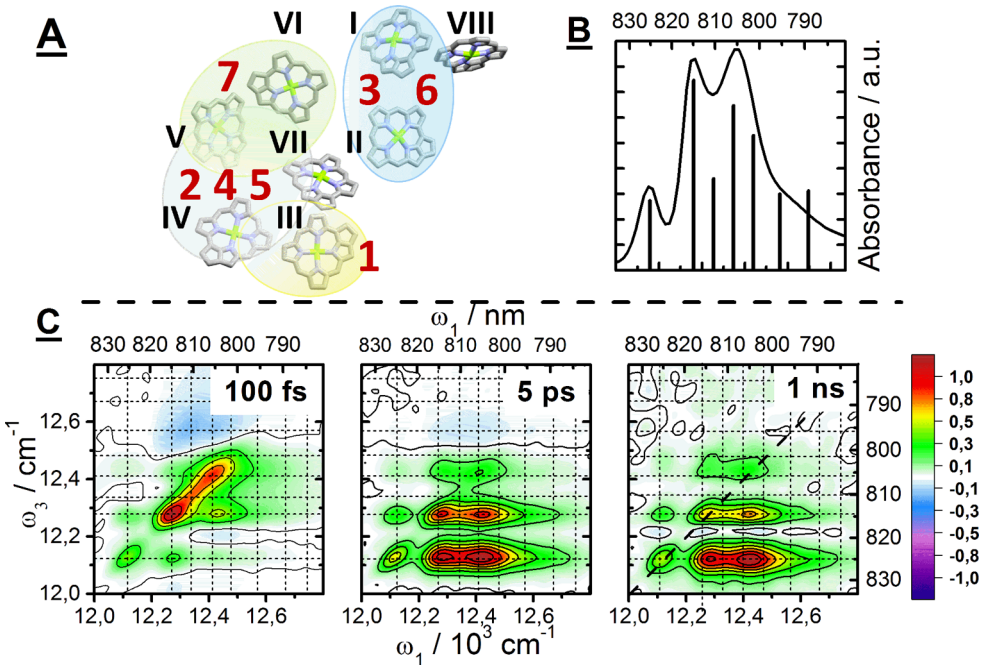

Figure 1. (A) Arrangement of BChl *a* pigments within the FMO units. BChl site numbering according to Fenna is in black Roman numerals. Schematic representation of spatial extent of the excitons according to Adolphs et al.[11] is shown by shaded areas. Exciton numbering (red numbers) is given in order of increasing energy. (B) linear absorption spectrum of FMO at 77 K with excitonic transitions (vide infra) represented by vertical bars. (C) Normalized absorptive 2D spectra at increasing population delays with dashed lines indicating excitonic transition energies. All spectra were recorded in 1:2 aqueous buffer:glycerol mixture at 77 K.

nm and spanning some 40 nm, rather than the 780 nm band observed for BChl in solution.[14] *Inter*unit coupling in the trimer on the other hand is relatively weak (below 20 cm^{-1} for all BChl pairs);[15,16] thus, the short time optical response is that of the individual subunits rather than of the protein complex as a whole. As a result, the spectrum of FMO contains observable features originating from a system of 7 (or 8) excitons rather than of 21 (or 24) excitons one would expect with stronger *inter*unit interaction. The energy spacing of the excitonic levels is relatively small (in the order of 5 nm), and the optical transitions show considerable inhomogeneous broadening, which results in severely congested spectra. The resulting linear absorption (LA) spectrum is almost entirely featureless at physiological temperatures, but at cryogenic temperatures, three distinct peaks emerge. In the FMO species investigated here, isolated from *Chlorobaculum tepidum*, these are found at 12 120 cm^{-1} (825 nm), 12 270 cm^{-1} (815 nm), and at 12 420 cm^{-1} (805 nm), while an additional broad shoulder is found on the blue side at approximately 12 650 cm^{-1} (790 nm).

The properties of FMO have been addressed with an array of optical techniques, ranging from steady-state absorption and fluorescence[3,17] to spectral hole-burning[18,19] and a variety of pump−probe-based techniques.[20−22] Nevertheless, the combination of closely spaced energy levels and rapid energy transfer leaves FMO as a difficult sample to probe by conventional time-resolved techniques. The direct relationship between spectral bandwidth and pulse length implies that either spectral or temporal resolution must be sacrificed. It presents, however, a well-suited system for two-dimensional electronic spectroscopy (2DES).

2DES was first implemented in the visible range in the end of the 1990s,[23−26] and has since proven to be a powerful time-resolved spectroscopy technique. The main strength of 2DES is its interferometric nature, relying on pumping by two interfering optical pulses followed by a single pulse, the "probe". This three-pulse (plus a *local oscillator*) sequence enables the acquisition of a two-dimensional map with high spectral resolution in both "pump" and "probe" frequency axes for each population time without sacrificing high temporal resolution. Thus, experiments are typically done using pulses of a few tens of femtoseconds or shorter. A particularly important demonstration of the capabilities of 2DES for studying complex systems was the visualization of electronic couplings in FMO isolated from *C. tepidum*.[27] This early study addressed the issue of correlations between states in the FMO electronic structure; however, theoretical modeling[12] resulted in only qualitative agreement with experimental data, and no attempt at quantifying energy-transfer rates or exciton correlations directly from experimental data were made. Subsequent work has focused primarily on the coherent response of the system;[5,6] thus, an accurate experimental determination of electronic structure and population dynamics was lacking. Here we revisit the problem of electronic structure and relaxation dynamics in this protein complex with the help of polarization controlled high-resolution 2DES. We thus record 2D spectra using the magic-angle pulse sequence ⟨54.7°, 54.7°, 0°, 0°⟩, where the sequence of four pulses of linear polarization angle Φ_i is denoted by $\langle\Phi_1, \Phi_2, \Phi_3, \Phi_4\rangle$ over a broad range of population times (femtoseconds up to a nanosecond) covering the entire excited-state lifetime window. Supplementary linear polarization schemes were used for detailed exciton structure determination, as described below. In total, these extensive data sets allow for, by use of an in-house developed global-fitting routine, accurate analysis of the energy-transfer processes in the excitonic state space.

We performed all experiments at cryogenic temperatures in the interest of obtaining a high degree of spectral resolution. Magic angle absorptive (real part of the signal) 2D spectra

DOI: 10.1021/acs.jpclett.6b00534
J. Phys. Chem. Lett. 2016, 7, 1653−1660

recorded at 77 K and at a range of representative population times are shown in Figure 1C. Representative 2D spectra at higher cryogenic temperatures can be found in the Supporting Information. The three main diagonal peaks in the short population time (100 fs) 2D spectrum are in good agreement both energetically and in shape with the corresponding features in LA and transient absorption spectra.[28]

A number of positive off-diagonal features, so-called cross-peaks, are observed in the 2D spectra. These correlate to excitonic states on the diagonal, where above-diagonal features indicate shared ground-state bleach (GSB), and below-diagonal features in addition contain stimulated emission (SE) signals, reporting on downward energy transfer.[23,27]

In an extended excitonic system such as FMO, shared GSB in particular implies some spatial overlap of excitonic wave functions, which allows us to qualitatively discuss also the spatial extent of the excitons. In FMO, all major diagonal features are connected by above-diagonal cross-peaks, indicating a large degree of spatial overlap of excitons and thus significant delocalization. Most simulations suggest delocalization over 2−3 BChl *a* sites for each exciton, e.g., the calculations by Adolphs and Renger[11] suggest spatial overlap between excitons **1**, **2**, **4**, and **5** at BChl *a* site IV (using Fenna's numbering). This situation is schematically illustrated in Figure 1A and is qualitatively consistent with our results. We note that exciton delocalization in FMO has been observed through shared GSB contributions also in transient absorption experiments.[21,28]

While the 2D diagonal contains all optically active states in the system, the diagonal trace appears similar to the LA spectrum; thus, assignment of the excitonic structure from this alone is impossible for FMO because of spectral congestion. The cross-peak spectral regions are often less congested, making 2DES very helpful in excitonic structure investigations because cross-peaks appear at coordinates directly corresponding to the energy of correlated exciton pairs. In many cases the energies (and correlations) of excitonic states can thus be simply read from the cross-peak coordinates. While this type of analysis is straightforward, in the case of FMO the considerable spectral congestion inhibits clear analysis even for such a procedure. A particularly large problem is the dominating diagonal signals, which hide or distort many of the relevant cross-peaks. A well-established approach for reducing congestion in linear and nonlinear spectra is exploiting polarization techniques.[29−32] We here modify Albrechts approach for separation of fluorescence excitation spectra into orthogonal components parallel and perpendicular to the emission.[32,33] The 2D analogue to this approach separates the spectrum into two components, polarized parallel and perpendicular to the "pumped" transition. The 2D diagonal, being pump and probe interaction with identical pulses, and cross peaks between states of small relative projection angles are selectively amplified in the former ($\mathbf{S}_Z$), while the latter ($\mathbf{S}_Y$) removes the diagonal entirely (and enhances cross-peaks at large projection angles), greatly reducing the spectral congestion. We note that somewhat conceptually different approaches to generate spectra proportional to $\mathbf{S}_Y$ have been taken by Zanni et al.[34] and Abramavicius et al.[35] Fleming and co-workers adapted the approach of Hochstrasser to 2DES,[36] using the "cross-peak specific" pulse sequence $\mathbf{S}_{\mathbf{CPS}} = \left\langle \frac{\pi}{3}, -\frac{\pi}{3}, 0, 0, \right\rangle$, which is directly proportional to $-\mathbf{S}_Y$. Because there is no direct way to apply the projection theorem[23] to assign absolute phase to $\mathbf{S}_{\mathbf{CPS}}$, we prefer to use the expressions detailed below. Further comparisons and discussion of these approaches can be found in the Supporting Information. In the present approach, we record the two polarized spectra $S_V = \langle 0, 0, 0, 0\rangle$ and $S_H = \left\langle \frac{\pi}{2}, \frac{\pi}{2}, 0, 0 \right\rangle$. From these experimental spectra we generate polarization associated spectra (PAS) from the expressions[32,33]

$$\mathbf{S}_Z = \frac{1}{3}(S_V + 2S_H)\left(5\frac{S_V - S_H}{S_V + 2S_H} + 1\right) = \mathrm{MA}(5r_0 + 1)$$

$$\mathbf{S}_Y = \frac{1}{3}(S_V + 2S_H)\left(2 - 5\frac{S_V - S_H}{S_V + 2S_H}\right) = \mathrm{MA}(2 - 5r_0)$$

Here MA is the spectrum recorded at the magic angle conditions and r_0 is the 2D analogue to the fluorescence (or pump−probe) anisotropy. Representative PAS maps at two temporally well-separated times are shown in Figure 2. The

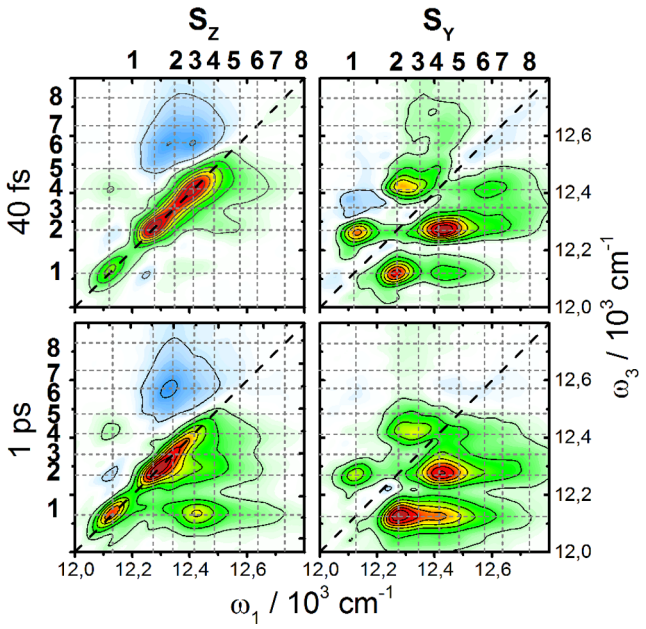

Figure 2. Normalized polarization associated spectra $\mathbf{S}_Z$ (left) and $\mathbf{S}_Y$ (right) at 40 fs (top row) and 1 ps (bottom row) population time. Gridlines correspond to the exciton energies derived from the cross-peak analysis and are labeled according to the exciton numbering used in the text.

decomposition of the total spectrum into two orthogonal components substantially reduces spectral congestion and allows for the cross-peak positions to be determined unambiguously by the simple cross-peak "triangulation" approach outlined above (exciton energy identification is shown explicitly in Figure S2). The resulting excitonic energy levels are shown as gridlines in the spectra in Figure 2, where individual cross- (and diagonal-) peaks can be found at the grid vertices.

The excitonic energies extracted from our analysis, listed in Table 1, are generally in good agreement with those derived by simultaneous fits to multiple spectra by Vulto et al.[22] We find significant disagreement only in the energy of exciton **6**. The somewhat higher energy derived from their procedure is likely due to the strong overlap of the spectrally broad transitions of

DOI: 10.1021/acs.jpclett.6b00534
J. Phys. Chem. Lett. 2016, 7, 1653−1660

Table 1. Energy-Transfer Rates between Excitonic States[a]

	|7⟩	|6⟩	|5⟩	|4⟩	|3⟩	|2⟩	E_n
|7⟩	**−29.9**	–	–	–	–	–	12.67
|6⟩	1.4	**−16.4**	–	–	–	–	12.57
|5⟩	6.4	–	**−5.1**	–	–	–	12.48
|4⟩	16.0	7.6	1.5	**−3.9**	–	–	12.41
|3⟩	6.1	2.4	1.2	–	**−0.83**	–	12.34
|2⟩	–	6.2	2.2	1.6	0.65	**−2.7**	12.27
|1⟩	–	–	–	1.3	–	2.3	12.12

[a]Transfer rates (population decay negative, population grow-in positive) in units of ps^{-1}. Upward transfer rates and rates contributing <5% of the level decay are omitted for clarity. Energies of the excitons (in 10^3 cm^{-1}) are found in the right-most column of the corresponding row.

excitons **6** and **7**, which are not clearly separable in linear and transient absorption spectra, making assignment from fitting of spectra difficult.

In agreement with the spectral structure of the 2D spectra in Figure 1, the cross-peak pattern in the PAS spectra implies an excitonic structure with strong correlation between most transitions. A notable exception is found for the cross-peak correlation pattern of exciton **3**: here, a number of high-energy cross-peaks are observed, but above-diagonal cross-peaks with any *lower* energy excitons are absent, implying spatial separation from the bottom of the FMO energy ladder. The spatial isolation of this exciton has been theoretically predicted[11] as a result of strong localization of exciton **3** at BChl sites I and II, where the partially overlapping excitons **1**−**5** (located at BChl sites III, IV, V, and VII) have negligible probability density. This situation is schematically illustrated in Figure 1A.

Close examination of the S_Y PAS spectrum in Figure 2 reveals two weak off-diagonal features, which appear as (above- and below-diagonal) cross-peaks corresponding to a correlation between exciton **3** and a state in the 12 700−12 750 cm^{-1} (~785 nm) spectral region. To our knowledge no experimental observation of such a high-energy state has been reported; however, the estimated energy agrees with the predictions by Schmidt am Busch et al.[8] for the exciton localized primarily on the recently discovered BChl 8 (other assignments of the spectral contribution of this exciton can be found in literature, e.g., Bina and Blankenship[7]). Following the work of Olbrich et al.[9] and Adolphs and Renger,[11] the strongest correlation of the high-energy exciton (mostly BChl 8) with exciton **3** implies that it is spatially close to BChl sites I and II, but on the *neighboring* unit in the FMO trimer. While the spectral signature in the PAS maps is clear, we note that the small oscillator strength of this transition, likely due to a very small population of BChl 8 in isolated FMO, renders it as only a minor contributor to the absorption spectrum.

With the exciton energies and their correlations in place, we can now analyze the details of energy transfer through the complex. With increasing population time the downward flow of energy through FMO is observed as shifting of the SE signal amplitude from the higher-energy diagonal peaks to lower-energy cross-peaks and as line shape changes. This overall relaxation can be separated into three distinct "stages", characterized by different time scales. The initial *intra*unit relaxation can be observed as the movement of SE signal from higher-energy states to the lowest exciton **1** and proceeds on a largely subpicosecond time scale. After a few picoseconds this transfer is complete, leaving the distinctive "streaked" spectral structure characteristic of shared GSB systems, illustrated by the 2D spectrum at 5 ps population time shown in Figure 1C. However, rounding of the initially strongly diagonally elongated lineshapes is fully completed only after approximately 100 ps, indicating a strong memory of initial excitation frequency of the system. These subtle spectral changes can be seen by comparison of the spectra at 5 ps and 1 ns in Figure 1C. The dynamics of these line shape changes can be extracted by analysis of decay-associated spectra (DAS), where the spectral shape time-evolution appears as a slow component well-separated from *intra*unit energy-transfer processes (see Supporting Information for DAS spectra). At 77 K, this analysis yields a rate of a few tens of picoseconds for these dynamics, in reasonable agreement with the spectral decay components assigned to *inter*unit energy transfer in low-temperature spectral hole-burning[19,37] and pump−probe[38] experiments. Following *intra*unit energy transfer and line shape changes, the remaining spectrum decays without further changes on a time scale of nanoseconds, consistent with the fluorescence lifetime (approximately 2 ns, using red-edge excitation[39]).

Quantitative characterization of the individual transfer steps in this highly complex overall relaxation network is challenging. However, it can be made tractable because the observations above approximately reduce the full relaxation dynamics to three independent stages: (1) *intra*unit relaxation in exciton manifold of seven states, (2) *inter*unit relaxation in an inhomogeneous distribution of "exciton **1** states", and (3) ground-state recovery. We focus here in particular on the first *intra*unit energy-transfer processes because the short time relaxation has been the most challenging for the traditional techniques.

Two-dimensional spectra can essentially be viewed as a two-dimensional matrix of kinetic traces. Such an extensive set of kinetic data obviously lends itself well to global analysis and global fitting approaches. The most common such approach, using decay associated spectra of sum-of-exponentials kinetic fits, is comparatively simple and often highly illuminating. However, it is only quantitatively useful in systems where the component lifetimes are very well-separated.[40] In the case of *intra*unit relaxation in FMO, a large number of transfer processes appear with similar rates, resulting in significant crosstalk between the parameters in a global DAS fit. It thus yields only qualitative information in this time regime, and only a "collective" subpicosecond component appears, which cannot be reliably separated into its individual constituents (a four-component DAS fit can be found in the Supporting Information).

Quantitative analysis of the initial relaxation processes in FMO clearly requires a different approach. Here we take advantage of the detailed knowledge about excitonic state energies and connectivity derived from the PAS spectra to directly impose a realistic physical model to the data. This allows the construction of a set of coupled differential equations, from which the transition rate constants can be extracted directly by fitting to the experimental data. Our routine globally fits GSB+ESA and SE contributions to all points in the 2D spectra simultaneously with the constraint of the assumed model, requiring only the input of the laser spectrum, temperature, number of states, and approximate line widths as initial conditions. Details of this routine are given in the Supporting Information. To improve convergence of the fitting procedure, we use as starting conditions the exciton

DOI: 10.1021/acs.jpclett.6b00534
J. Phys. Chem. Lett. 2016, 7, 1653−1660

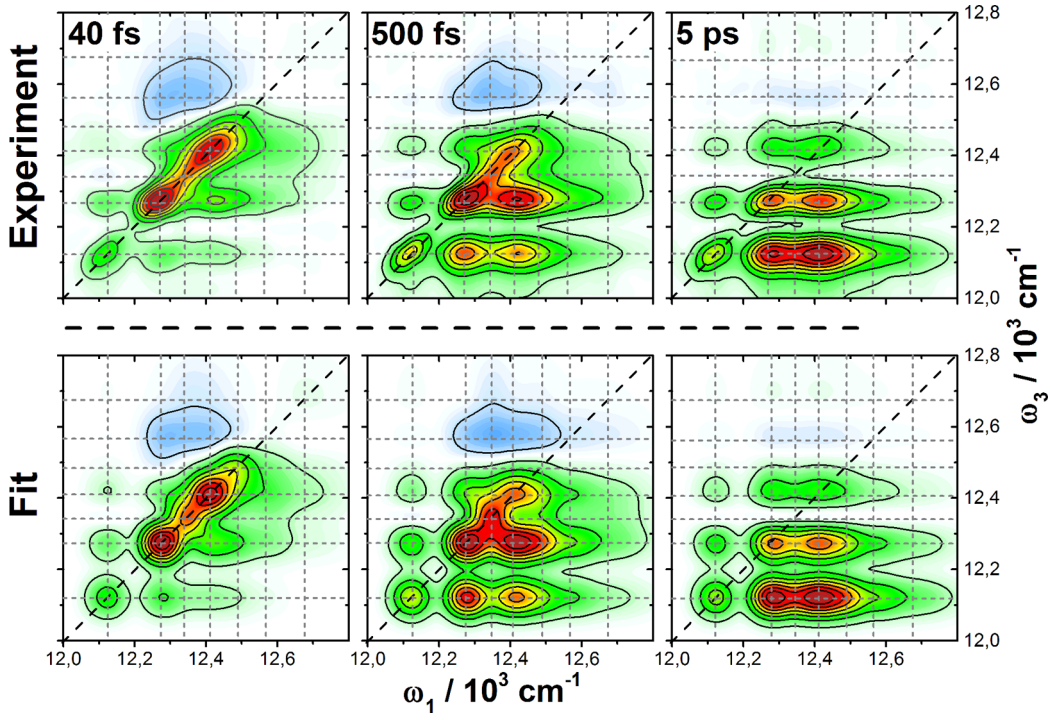

Figure 3. Comparison of normalized experimental 2D spectra (top row) and 2D spectra calculated from the kinetic fit (bottom row) at three population times. Gridlines correspond to the excitonic energy.

energies extracted from the PAS maps and the assumption that the largest transition rates from a given excitonic level are connected to transitions between spatially overlapping excitons (as seen by the presence of above-diagonal cross-peaks). We further ignore BChl 8 in these fits because it contributes negligibly to the observed photoinduced dynamics because of its weak absorption. With these starting parameters we can extract all state-to-state transfer rates by a simultaneous fit of the 2D spectra at all population times with reproduction of the LA spectrum as an additional constraint. Comparison between a few experimental 2D spectra and spectra extracted from the fit are shown in Figure 3, and the resulting model is summarized in the transition matrix in Table 1 and the schematic illustration in Figure 4.

The rates extracted here agree qualitatively with those determined in transient absorption experiments,[20−22,28] in that *intra*unit energy transfer is found to proceed largely on subpicosecond time scales and that higher-energy excitons are extremely short-lived. However, accurate kinetics have not been available from these earlier studies, because the exciton lifetimes are comparable to or shorter than the excitation pulses used in several cases. Furthermore, deconvolution of the observed decays into individual energy-transfer steps could not be easily effected because of the large number of transitions necessarily covered by the finite-width laser spectra. Both these issues are circumvented in 2DES, which lets us use pulses that are substantially shorter than the exciton lifetimes and observe the level-to-level transfer times directly in the cross-peak dynamics. While 2DES literature on FMO is substantial, to date these highly advantageous characteristics have not been used for quantitative experimental characterization of the energy-transfer network in FMO.

As illustrated in Figure 4 and Table 1, it is apparent that there is some "branching" in the relaxation, in that, for example, exciton **6** preferentially relaxes via exciton **4** and not **5**. Overall,

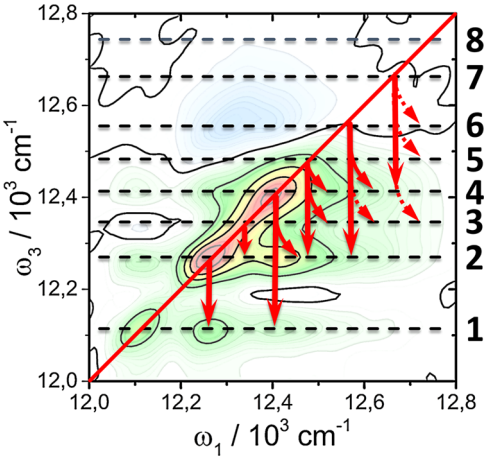

Figure 4. Two-dimensional spectrum at 100 fs delay with excitonic levels indicated with dashed lines. A schematic illustration of the relaxation cascade is inserted. Solid arrows indicate channels responsible for a large relative fraction of the total transfer from a given level, while dashed arrows indicate minor channels.

however, we observe complex and strongly interconnected relaxation processes. While it is clear that the spatial overlap of excitons influences the magnitude of individual transition rates in the relaxation, our data do not support the model of two spatially separated relaxation pathways through the complex suggested in early 2DES work.[12,27,41] Instead, we observe a "multi-branching", interconnected network of transfer pathways where each state may transfer its population into a number of other states. The discrepancy between the extracted models likely originates from the qualitative nature of earlier 2DES work on population dynamics, where only a select few "snapshots" of the population decay were measured.

DOI: 10.1021/acs.jpclett.6b00534
J. Phys. Chem. Lett. 2016, 7, 1653−1660

An exception to the otherwise rapid *intra*unit dynamics is the picosecond time scale relaxation of exciton **3**. Transfer to this state from other states occurs with relatively low probability and depopulation is slow; thus, it poses a "semi-trap" in the otherwise fast and efficient energy-transfer network. The weak connection of this exciton to the rest can be understood from the lack of correlation with lower-energy states in the "energy ladder". This implies some degree of spatial isolation from its energetically favorable decay channels, in agreement with earlier calculations,[11] which in turn intuitively suggests a smaller relaxation rate. Though this slow kinetic component has been observed in transient absorption kinetics,[22,42] the significance of such a trap to the operation of native FMO is unclear. The relatively low probability of population and slow deactivation implies a minor, if any, role in the function of the complex.

The *inter*unit energy transfer, apparent in the line shape dynamics after completion of the initial relaxation to exciton **1**, appear simply as an additional component in the kinetic traces at long times. However, it was omitted here for clarity. Regardless of whether the rate of this process is extracted by line shape changes, DAS, or rate constant fitting, it appears with a rate constant of approximately 3.5×10^{-2} ps^{-1}, in qualitative agreement with *inter*unit energy-transfer rates estimated from liquid helium temperature spectral hole-burning[19,37] and pump−probe measurements.[38]

In summary, we have shown that the high spectral- and temporal- resolution of 2DES in combination with a decomposition of the total spectrum into orthogonal PAS maps allows the emergence of a complete and consistent picture of both the electronic structure and the energy-transfer kinetics in FMO at low temperatures. The selective suppression of the strongly "diagonal" spectral contributions further allowed the first experimental observation of the exciton primarily situated on the recently discovered elusive BChl 8. Furthermore, we demonstrate that the large amount of spectrally well-resolved kinetic data inherently present in a typical 2DES data set forms an ideal basis for advanced global fitting procedures. The complex, interconnected seven-state relaxation in FMO was thus resolved into a matrix of level-to-level transfer rates by use of an in-house developed fitting tool. This resulting transfer matrix of multibranching pathways represents a considerable refinement to the present model of the excited-state relaxation in FMO. Finally, we note that the approach of direct-fitting-of-rates to sets of 2DES and LA spectra taken here is general and can be applied to a wide array of systems in which exponential kinetics models are applicable. In particular, this can prove beneficial in the analysis of complex systems, where ambiguities in fits of pump−probe data may hinder the construction of a reliable and meaningful physical model of the relaxation dynamics.

EXPERIMENTAL SECTION

Details on bacteria culture growth and FMO isolation procedures are given in the Supporting Information.

All measurements were done in a standard cryogenic buffer containing a 1:2 ratio of aqueous buffer:glycerol. The sample was kept in a demountable 0.5 mm path length fused silica cell, supported in a temperature-controlled liquid nitrogen bath cryostat (Optistat DN2, Oxford Instruments) equipped with fused silica windows. The maximum optical density in the probed spectral window was kept between 0.1 and 0.3 in all experiments. Linear absorption spectra were recorded, in the cryostat, on a PerkinElmer lambda 1050 UV/vis/NIR spectrometer.

The 2DES setup is described in detail elsewhere;[43] we briefly summarize key points here: A 1027 nm centered Pharos (Light Conversion ltd.) laser is used to pump a noncollinear optical amplifier (Light Conversion ltd.), the output of which is compressed by a fused silica prism compressor. The resulting output is approximately 14 fs, ∼80 nm full width at half-maximum pulses with a spectrum centered at 805 nm. The pulse energy was 1.5 nJ or 750 nJ, and the experiment was done at a 5 kHz repetition rate. The coherence time was scanned from −270 to +450 fs in 1.8 fs steps, resulting in a spectral resolution of 37 cm^{-1} on the ω_1 axis.

To avoid depolarization artifacts in the population dynamics, we record spectra at the magic angle polarization conditions ⟨54.7, 54.7, 0, 0⟩. Here, each number corresponds to the polarization angle of the three exciting pulses and analyzer. Additional spectra were recorded with ⟨0, 0, 0, 0⟩ and ⟨90, 90, 0, 0⟩ polarization conditions to generate PAS spectra. Proper phase of the measured 2D spectra were in all cases determined by comparison of 2D projection with pump−probe spectra recorded under the same conditions.[23] 2DES spectra are recorded at a range of population times over several measurement series, with a typical series containing 50−100 2D spectra. The total measured population times span the range from 0 fs to 1 ns. We assess the quality of the 2D spectra by extracting transient absorption spectra and comparing this with literature data. Overall, we find good agreement. During the acquisition we observed slight selective bleaching of exciton 2, which necessitated the use of low-intensity pulses and low repetition rates. Careful control of the conditions let us keep the bleaching of this peak <5% over a 120 population time point measurement, while the bleaching was negligible during the exciton 2 lifetime.

Kinetic analysis was done by simultaneous fitting the kinetics in all points in the 2DES map, using a combination of the Levenberg−Marquardt algorithm and particle swarm optimization. The quality of the fits were assessed by χ^2 analysis and visual comparison of the extracted 2DES and LA spectra with their experimental counterparts. For more details, see the Supporting Information.

ASSOCIATED CONTENT

Supporting Information

The Supporting Information is available free of charge on the ACS Publications website at DOI: 10.1021/acs.jpclett.6b00534.

FMO extraction procedures, high-cryogenic temperature 2D spectra, details on PAS generation, 2D-DAS spectra, and details on fitting procedure (PDF)

AUTHOR INFORMATION

Corresponding Author

*E-mail: donatas.zigmantas@chemphys.lu.se.

Notes

The authors declare no competing financial interest.

ACKNOWLEDGMENTS

E.T., K.Z., and D.Z. acknowledge support from the Knut & Alice Wallenberg foundation and Swedish Research Council. D.B. acknowledges support by Czech Science Foundation under Grant P501/12/G055 and institutional support RVO:60077344. J.D. thanks the DFG for funding within the

DOI: 10.1021/acs.jpclett.6b00534
J. Phys. Chem. Lett. 2016, 7, 1653−1660

Research Unit "Light-induced dynamics in molecular aggregates" (FOR1809).

REFERENCES

(1) Fenna, R. E.; Matthews, B. W. Chlorophyll Arrangement in a Bacteriochlorophyll Protein from Chlorobium-Limicola. *Nature* **1975**, *258*, 573−577.

(2) Tronrud, D. E.; Wen, J. Z.; Gay, L.; Blankenship, R. E. The Structural Basis for the Difference in Absorbance Spectra for the Fmo Antenna Protein from Various Green Sulfur Bacteria. *Photosynth. Res.* **2009**, *100*, 79−87.

(3) Milder, M. T. W.; Bruggemann, B.; van Grondelle, R.; Herek, J. L. Revisiting the Optical Properties of the Fmo Protein. *Photosynth. Res.* **2010**, *104*, 257−274.

(4) Savikhin, S.; Buck, D. R.; Struve, W. S. Oscillating Anisotropies in a Bacteriochlorophyll Protein: Evidence for Quantum Beating between Exciton Levels. *Chem. Phys.* **1997**, *223*, 303−312.

(5) Engel, G. S.; Calhoun, T. R.; Read, E. L.; Ahn, T. K.; Mancal, T.; Cheng, Y. C.; Blankenship, R. E.; Fleming, G. R. Evidence for Wavelike Energy Transfer through Quantum Coherence in Photosynthetic Systems. *Nature* **2007**, *446*, 782−786.

(6) Panitchayangkoon, G.; Hayes, D.; Fransted, K. A.; Caram, J. R.; Harel, E.; Wen, J. Z.; Blankenship, R. E.; Engel, G. S. Long-Lived Quantum Coherence in Photosynthetic Complexes at Physiological Temperature. *Proc. Natl. Acad. Sci. U. S. A.* **2010**, *107*, 12766−12770.

(7) Bina, D.; Blankenship, R. E. Chemical Oxidation of the Fmo Antenna Protein from Chlorobaculum Tepidum. *Photosynth. Res.* **2013**, *116*, 11−19.

(8) Schmidt am Busch, M.; Muh, F.; Madjet, M. E.; Renger, T. The Eighth Bacteriochlorophyll Completes the Excitation Energy Funnel in the Fmo Protein. *J. Phys. Chem. Lett.* **2011**, *2*, 93−98.

(9) Olbrich, C.; Jansen, T. L. C.; Liebers, J.; Aghtar, M.; Strumpfer, J.; Schulten, K.; Knoester, J.; Kleinekathofer, U. From Atomistic Modeling to Excitation Transfer and Two-Dimensional Spectra of the Fmo Light-Harvesting Complex. *J. Phys. Chem. B* **2011**, *115*, 8609−8621.

(10) Olbrich, C.; Strumpfer, J.; Schulten, K.; Kleinekathofer, U. Theory and Simulation of the Environmental Effects on Fmo Electronic Transitions. *J. Phys. Chem. Lett.* **2011**, *2*, 1771−1776.

(11) Adolphs, J.; Renger, T. How Proteins Trigger Excitation Energy Transfer in the Fmo Complex of Green Sulfur Bacteria. *Biophys. J.* **2006**, *91*, 2778−2797.

(12) Cho, M. H.; Vaswani, H. M.; Brixner, T.; Stenger, J.; Fleming, G. R. Exciton Analysis in 2d Electronic Spectroscopy. *J. Phys. Chem. B* **2005**, *109*, 10542−10556.

(13) Vulto, S. I. E.; de Baat, M. A.; Louwe, R. J. W.; Permentier, H. P.; Neef, T.; Miller, M.; van Amerongen, H.; Aartsma, T. J. Exciton Simulations of Optical Spectra of the Fmo Complex from the Green Sulfur Bacterium Chlorobium Tepidum at 6 K. *J. Phys. Chem. B* **1998**, *102*, 9577−9582.

(14) Ratsep, M.; Cai, Z. L.; Reimers, J. R.; Freiberg, A. Demonstration and Interpretation of Significant Asymmetry in the Low-Resolution and High-Resolution Q(Y) Fluorescence and Absorption Spectra of Bacteriochlorophyll A. *J. Chem. Phys.* **2011**, *134*, 024506.

(15) Louwe, R. J. W.; Vrieze, J.; Hoff, A. J.; Aartsma, T. J. Toward an Integral Interpretation of the Optical Steady-State Spectra of the Fmo-Complex of Prosthecochloris Aestuarii. 2. Exciton Simulations. *J. Phys. Chem. B* **1997**, *101*, 11280−11287.

(16) Pearlstein, R. M. Theory of the Optical-Spectra of the Bacteriochlorophyll-a Antenna Protein Trimer from Prosthecochloris-Aestuarii. *Photosynth. Res.* **1992**, *31*, 213−226.

(17) Wendling, M.; Przyjalgowski, M. A.; Gulen, D.; Vulto, S. I. E.; Aartsma, T. J.; van Grondelle, R.; van Amerongen, H. The Quantitative Relationship between Structure and Polarized Spectroscopy in the Fmo Complex of Prosthecochloris Aestuarii: Refining Experiments and Simulations. *Photosynth. Res.* **2002**, *71*, 99−123.

(18) Franken, E. M.; Neerken, S.; Louwe, R. J. W.; Amesz, J.; Aartsma, T. J. A Permanent Hole Burning Study of the Fmo Antenna Complex of the Green Sulfur Bacterium Prosthecochloris Aestuarii. *Biochemistry* **1998**, *37*, 5046−5051.

(19) Ratsep, M.; Blankenship, R. E.; Small, G. J. Energy Transfer and Spectral Dynamics of the Three Lowest Energy Q(Y)-States of the Fenna-Matthews-Olson Antenna Complex. *J. Phys. Chem. B* **1999**, *103*, 5736−5741.

(20) Savikhin, S.; Struve, W. S. Ultrafast Energy-Transfer in Fmo Trimers from the Green Bacterium Chlorobium-Tepidum. *Biochemistry* **1994**, *33*, 11200−11208.

(21) Buck, D. R.; Savikhin, S.; Struve, W. S. Ultrafast Absorption Difference Spectra of the Fenna-Matthews-Olson Protein at 19 K: Experiment and Simulations. *Biophys. J.* **1997**, *72*, 24−36.

(22) Vulto, S. I. E.; de Baat, M. A.; Neerken, S.; Nowak, F. R.; van Amerongen, H.; Amesz, J.; Aartsma, T. J. Excited State Dynamics in Fmo Antenna Complexes from Photosynthetic Green Sulfur Bacteria: A Kinetic Model. *J. Phys. Chem. B* **1999**, *103*, 8153−8161.

(23) Jonas, D. M. Two-Dimensional Femtosecond Spectroscopy. *Annu. Rev. Phys. Chem.* **2003**, *54*, 425−463.

(24) Mukamel, S. Multidimensional Femtosecond Correlation Spectroscopies of Electronic and Vibrational Excitations. *Annu. Rev. Phys. Chem.* **2000**, *51*, 691−729.

(25) Hybl, J. D.; Albrecht, A. W.; Faeder, S. M. G.; Jonas, D. M. Two-Dimensional Electronic Spectroscopy. *Chem. Phys. Lett.* **1998**, *297*, 307−313.

(26) Hybl, J. D.; Ferro, A. A.; Jonas, D. M. Two-Dimensional Fourier Transform Electronic Spectroscopy. *J. Chem. Phys.* **2001**, *115*, 6606−6622.

(27) Brixner, T.; Stenger, J.; Vaswani, H. M.; Cho, M.; Blankenship, R. E.; Fleming, G. R. Two-Dimensional Spectroscopy of Electronic Couplings in Photosynthesis. *Nature* **2005**, *434*, 625−628.

(28) Vulto, S. I. E.; Neerken, S.; Louwe, R. J. W.; de Baat, M. A.; Amesz, J.; Aartsma, T. J. Excited-State Structure and Dynamics in Fmo Antenna Complexes from Photosynthetic Green Sulfur Bacteria. *J. Phys. Chem. B* **1998**, *102*, 10630−10635.

(29) Thulstrup, E. W.; Eggers, J. H. Moment Directions of the Electronic Transitions of Fluoranthene. *Chem. Phys. Lett.* **1968**, *1*, 690−692.

(30) Michl, J.; Thulstrup, E. W. Ultraviolet and Infrared Linear Dichroism - Polarized-Light as a Probe of Molecular and Electronic-Structure. *Acc. Chem. Res.* **1987**, *20*, 192−199.

(31) Valeur, B.; Weber, G. Resolution of Fluorescence Excitation Spectrum of Indole into 1la and 1lh Excitation Bands. *Photochem. Photobiol.* **1977**, *25*, 441−444.

(32) Albrecht, A. C. Polarizations and Assignments of Transitions - Method of Photoselection. *J. Mol. Spectrosc.* **1961**, *6*, 84−104.

(33) Thyrhaug, E.; Sorensen, T. J.; Gryczynski, I.; Gryczynski, Z.; Laursen, B. W. Polarization and Symmetry of Electronic Transitions in Long Fluorescence Lifetime Triangulenium Dyes. *J. Phys. Chem. A* **2013**, *117*, 2160−2168.

(34) Zanni, M. T.; Ge, N. H.; Kim, Y. S.; Hochstrasser, R. M. Two-Dimensional Ir Spectroscopy Can Be Designed to Eliminate the Diagonal Peaks and Expose Only the Crosspeaks Needed for Structure Determination. *Proc. Natl. Acad. Sci. U. S. A.* **2001**, *98*, 11265−11270.

(35) Abramavicius, D.; Voronine, D. V.; Mukamel, S. Unravelling Coherent Dynamics and Energy Dissipation in Photosynthetic Complexes by 2d Spectroscopy. *Biophys. J.* **2008**, *94*, 3613−3619.

(36) Read, E. L.; Engel, G. S.; Calhoun, T. R.; Mancal, T.; Ahn, T. K.; Blankenship, R. E.; Fleming, G. R. Cross-Peak-Specific Two-Dimensional Electronic Spectroscopy. *Proc. Natl. Acad. Sci. U. S. A.* **2007**, *104*, 14203−14208.

(37) Kell, A.; Acharya, K.; Zazubovich, V.; Jankowiak, R. On the Controversial Nature of the 825 Nm Exciton Band in the Fmo Protein Complex. *J. Phys. Chem. Lett.* **2014**, *5*, 1450−1456.

(38) Vulto, S. I. E.; Streltsov, A. M.; Aartsma, T. J. Excited State Energy Relaxation in the Fmo Complexes of the Green Bacterium Prosthecochloris Aestuarii at Low Temperatures. *J. Phys. Chem. B* **1997**, *101*, 4845−4850.

(39) Zhou, W. L.; Lobrutto, R.; Lin, S.; Blankenship, R. E. Redox Effects on the Bacteriochlorophyll a-Containing Fenna-Matthews-

DOI: 10.1021/acs.jpclett.6b00534
J. Phys. Chem. Lett. 2016, 7, 1653−1660

Olson Protein from Chlorobium-Tepidum. *Photosynth. Res.* **1994**, *41*, 89−96.
(40) van Stokkum, I. H. M.; Larsen, D. S.; van Grondelle, R. Global and Target Analysis of Time-Resolved Spectra. *Biochim. Biophys. Acta, Bioenerg.* **2004**, *1657*, 82−104.
(41) Read, E. L.; Schlau-Cohen, G. S.; Engel, G. S.; Wen, J. Z.; Blankenship, R. E.; Fleming, G. R. Visualization of Excitonic Structure in the Fenna-Matthews-Olson Photosynthetic Complex by Polarization-Dependent Two-Dimensional Electronic Spectroscopy. *Biophys. J.* **2008**, *95*, 847−856.
(42) Savikhin, S.; Buck, D. R.; Struve, W. S. Toward Level-to-Level Energy Transfers in Photosynthesis: The Fenna-Matthews-Olson Protein. *J. Phys. Chem. B* **1998**, *102*, 5556−5565.
(43) Augulis, R.; Zigmantas, D. Two-Dimensional Electronic Spectroscopy with Double Modulation Lock-in Detection: Enhancement of Sensitivity and Noise Resistance. *Opt. Express* **2011**, *19*, 13126−13133.

DOI: 10.1021/acs.jpclett.6b00534
J. Phys. Chem. Lett. 2016, 7, 1653−1660